ISSN 1070-3632, Russian Journal of General Chemistry, 2008, Vol. 78, No. 5, pp. 868–875. © Pleiades Publishing, Ltd., 2008.
Original Russian Text © V.B. Kopylov, K.A. Aleksandrov, E.V. Sergeev, 2008, published in Zhurnal Obshchei Khimii, 2008, Vol. 78, No. 5, pp. 726–733.

Thermal Evolution of the Chemical Structure and Properties of Silicon Oxides

V. B. Kopylov, K. A. Aleksandrov, and E. V. Sergeev

Herzen Russian State Pedagogical University, nab. r. Moiki 48, St. Petersburg, 191186 Russia
e-mail: vladimir_kopylov@mail.ru

Received August 29, 2007

Abstract—High-resolution IR spectroscopic study has shown that stepwise heating of samples of silicon oxides in the temperature range from 50 to 1000°C is accompanied by accumulation of electronically excited states in the skeletal Si–O bond system, as well as by formation of associates in the cationic and anionic sublattices. Stationary association process and cooperative interaction of the excited states give rise to IR luminescence and diamagnetic response which increases as the temperature rises. Accumulation of the excited states in the chemical structure and their relaxation, including that occurring due to thermal desorption of singlet oxygen, are characterized by nonmonotonic temperature dependence of the heat capacity.

DOI: 10.1134/S1070363208050058

Specificity of the real structure and properties of silicon oxides are largely determined by the presence and association of bulk and surface defects [1, 2]. The chemical structure of the latter continues to attract a keen interest, for it determines the magnitude and character of catalytic activity, as well as the chemical origin of properties of one of the most widespread classes of materials. Usually, intrinsic defects are concerned, where a silicon atom is linked to three or two lattice oxygen atoms. The first of these are paramagnetic radical centers [E_s' (1) centers] $(–Si–O)_3Si^{\cdot}$ and $(–Si–O)_3SiO^{\cdot}$, while the second are diamagnetic silylene structures $(–Si–O)_2Si$**:**. They include several intrinsic diamagnetic defects where silicon atoms have different oxidation numbers. The main methods for identification of such structures are electron spin resonance (ESR) and electronic absorption and luminescence spectroscopy [2].

Using high-resolution IR spectroscopy we previously showed [3] that intrinsic defects in SiO_2 include dimeric and trimeric oxygen associates (O_2, O_2^-, $O_2^{\cdot -}$, O_3), as well as isolated Si–O and Si–Si oscillators in the ground and excited states, which are chemical products of redox process (one-electron transfer), i.e., electron–hole components of electronically excited states (Coulomb excitons); the latter strongly tend to undergo association and (after reaching a critical concentration) condensation-like cooperative interactions [4, 5]. The electronic structure of such states, their activity, and stabilization in microheterogeneous domains of real solids [6] imply that they could be identified at elevated temperature by vibrational spectroscopy and analysis of heat capacity and magnetic susceptibility of samples.

Study on variation of the state of skeletal bonds with rise in temperature showed that the intensity (optical density) at the centroid of the fundamental $\nu_{as(Si–O–Si)}$ band (~1100 cm^{-1}, A_1; Fig. 1) considerably and monotonically decreases in the range from 25 to 700°C. At 700°C, the bonds become vibrationally excited, giving rise to a luminescence peak. Simultaneously, extremal increase of vibrational activity is observed in the frequency range from 840 to 660 cm^{-1}, where the absorption pattern corresponds to the spectrum of electronically excited isolated Si–O oscillators ($A^1\Pi$, 840 cm^{-1}; $a^3\Sigma^+$, 782 cm^{-1}; $d^3\Delta_r$, 759 cm^{-1}; $e^3\Sigma^-$, 740 cm^{-1}; $D^1\Delta$, 722 cm^{-1}; $E^1\Sigma^+$, 667 cm^{-1}) [7].

These variations, as well as decrease in intensity and almost complete disappearance at 700°C of the Si–O band corresponding to the principal vibrational transition of the molecular state (1230 cm^{-1}, high-frequency anomaly [8]), suggest that the oxide structure ensures high efficiency of the transformation of vibrational (thermal) excitation into electronic and that highly excited states predominate above 300°C. This is consistent with the concept [9] on the contribution of

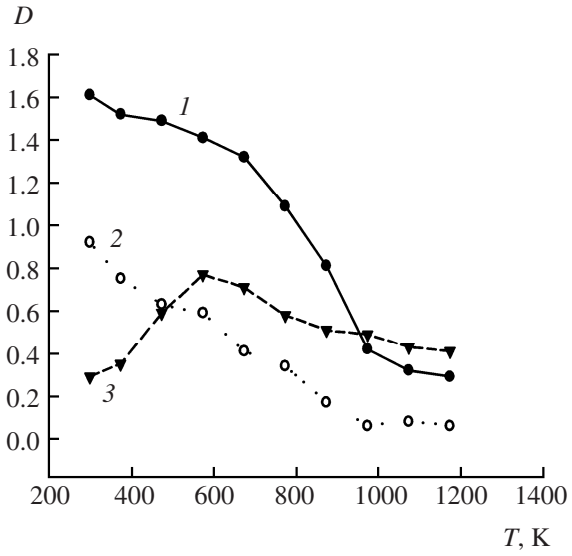

Fig. 1. Thermal evolution of optical density at frequencies corresponding to (*1*) skeletal vibrations (D_{1100}, Si–O–Si) and (*2*, *3*) molecular states of Si–O [(*2*) D_{1230}, $^1\Sigma^+$, $E_{ex} = 0$; (*3*) D_{780}, $^1\Sigma^+$, $E_{ex} = 4.0$] in the spectrum of A-300 aerosil.

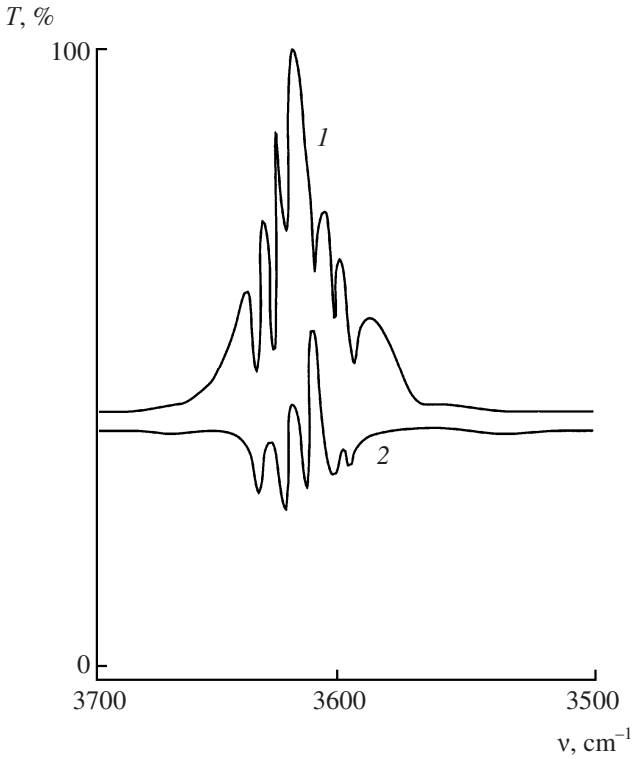

Fig. 2. Luminescence and absorption bands in the spectrum of A-300 aerosil at (*1*) 573 and (*2*) 973 K; *T* stands for transmittance.[1]

the electronic structure of the $[SiO_4]^{4-}$ polyhedron to the barriers along the relaxation path of vibrational perturbation energy. Simultaneously, the concentration of strained –Si–O–Si– bridging bonds increases; these bonds are characterized by a doublet at 888/908 cm^{-1} [10]. At a temperature above 500°C, the intensity of the characteristic absorption bands sharply decreases, and a broad structured band appears in the region 1000–900 cm^{-1} and increases in intensity. Insofar as the centroid of the band at 950–960 cm^{-1} is usually assigned [10] to stretching vibrations of –Si–O bonds where the oxygen atom is linked to only one silicon atom, in our case the reason may be formation of –Si–$O^{\cdot}$ radicals or –Si–$O^{\cdot-}$ radical ions.

The IR spectra of Aerosil A-300, silica gel, quartz, and quartz glass, recorded at elevated temperature, are characterized by the presence of a broad luminescence band centered at 3615 cm^{-1} (Fig. 2), whose intensity increases up to 773 K. In addition, a well resolved series of absorption bands appears on the background of the above band. Raising the temperature to 993 K is accompanied by transformation of that band into a narrow emission peak at 3607 cm^{-1} and strong absorption bands at 3640, 3625, and 3612 cm^{-1}. At the maximal temperature (1273 K), the luminescence intensity strongly decreases, but the absorption pattern is generally retained. According to Scheme (1) for the formation and association of exciton defects, the high-temperature luminescence bands could originate from vibrational relaxation processes and cooperative interactions (condensation), the latter leading to stabilization of the excited assotsiates.

$$n[SiO_2] \leftrightarrow n\mathrm{Si} + 2n\mathrm{O} \leftrightarrow \mathrm{Si}_n + \mathrm{O}_{2n}. \qquad (1)$$

It should be kept in mind that the position of absorption bands intrinsic to associates does not necessarily coincide with the position of the emission lines. The assignment of fine-structure absorption bands involves no difficulties, for the highest-frequency luminescence maxima at 3640 and 3625 cm^{-1} quite conform to stretching vibrations of hydroxy groups (O–H) perturbed by oxygen oligomers (associates) [10], and the band at 3612 cm^{-1} corresponds to stretching vibrations of the same bonds in hydrogen peroxide [12]. The intensity of the

[1] As in Russian original.

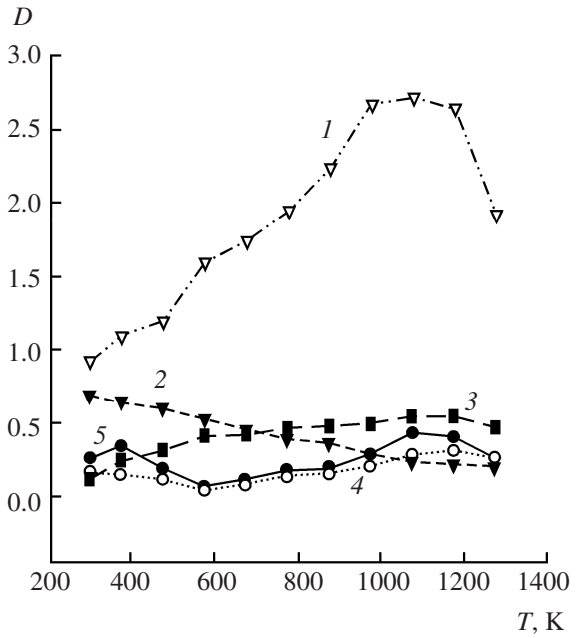

Fig. 3. Variation of optical density at characteristic frequencies in the spectrum of A-300 aerosil: (*1*) D_{505}, Si–Si; (*2*) D_{840}, Si–O; (*3*) D_{668}, O–O; (*4*) D_{1457}, $^1O_2$; and (*5*) D_{1557}, O_2.

Table 1. Positions of the experimental and calculated lines in the vibrational spectra of oxygen molecules and associates

Species	ν_{exp}, cm^{-1} (I_{max})	ν_{calc}, cm^{-1} (I_{max})
O_2 ($^3\Sigma_g^-$)	1556	1561
O_2 ($^1\Delta_g$)	1457	1492
O_2 ($^1\Sigma_g^+$)	1420	1437
O_2^+	1870	1777
O_2^-	1140–1180	1110
O_3	1040	1009
O_3^-	1020	997
O_2 ($^3\Sigma_g^-$)–O_2 ($^3\Sigma_g^-$)	1240	1254
O_2 ($^3\Sigma_g^-$)–O_2 ($^1\Delta_g$)	–	716
O_2 ($^3\Sigma_g^-$)–O_2 ($^1\Sigma_g^+$)	–	720
O_2 ($^1\Sigma_g^+$)–O_2 ($^1\Sigma_g^+$)	–	729
O_2 ($^1\Delta_g$)–O_2 ($^1\Delta_g$)	–	720
O_2 ($^1\Delta_g$)–O_2 ($^1\Sigma_g^+$)	–	724
O_2 ($^1\Delta_g$)–O_2^+	1750, 1240	1822, 1268
O_2 ($^1\Delta_g$)–O_2^-	1370	1468
O_2 ($^3\Sigma_g^-$)–O_2^+	1750, 1370	1754, 1361
O_2 ($^3\Sigma_g^-$)–O_2^-	1557	1555
O_2 ($^1\Sigma_g^+$)–O_2^+	1750, 1240	1745, 1268
O_2 ($^3\Sigma_g^-$)–O_2^-	1370	1427

stretching vibration band of hydroperoxide bonds (3600–3620 cm^{-1}) is related to the absorption intensity in the region 700–600 cm^{-1} (Fig. 3), where vibrational activity of peroxide groups on the SiO_2 surface is observed [13]. This assignment is consistent with the presence of bands at 2360 cm^{-1}, which belong to asymmetric stretching vibrations ν_{as} of CO_2 molecules tending to be strongly bound (via sorption forces) by peroxide groups [14]. Vibrational activity of O–OH peroxide type functional groups does not exclude the possibility for formation of compounds like hydrogen polyoxides H_2O_3 and H_2O_4 [12] and their structural analogs on the silicon oxide surface.

Enlargement of oxygen associates, which is reflected in increase in the enthalpy of condensation, and the related tendency of the force constant to increase should be accompanied by appearance and high-frequency shift of strong characteristic absorption bands. It is known [14] that ion clusters are considerably stronger than molecular clusters. The ΔH values for O_4^+ and O_4^- were estimated, respectively, at –40.3 (~3224 cm^{-1}) and –54.35 kJ mol^{-1} (~4348 cm^{-1}). These data are consistent with the high-frequency position of the observed luminescence band and with the results of quantum-chemical calculations [14], according to which O_4 ionic dimers are planar linear complexes. In order to verify our assignments, the vibrational activity of oxygen molecules and planar O_4 dimers was simulated using NDDO–AM1 semi-empirical approximation incorporated into Hypercube Hyperchem Professional v7.01 (Table 1).

Another remarkable specificity of the spectra was a series of absorption bands in the region 2060–2000 cm^{-1}, whose intensity increased as the temperature rose and reached its maximal value at 1273 K (Fig. 4). Almost complete absence of vibrational activity of most compounds in the above region under normal conditions raises a problem related to the nature of these absorption bands. Taking into account the probability of their combination or overtone origin, the role of excited states and association processes may be estimated. A probable size of associates that could give rise to absorption at 2060–2000 cm^{-1} corresponds to $[O]_5$–$[O]_8$. Computer simulation of the structure and vibrational activity of $[O]_5$–$[O]_8$ associates in the ionic and molecular states showed that the smallest negatively charged associate in this series, $[O]_5^-$, is characterized by the strongest line at 2006 cm^{-1} and less intense doublet at 1700 cm^{-1}; these frequencies agree well with the experimentally observed peaks at

2010, 2004, 1700, and 1690 cm^{-1}. The calculated spectrum of $[O]_8^-$ ion contains a strong line at 2060 cm^{-1} and concomitant bands at 1650 and 1680 cm^{-1}, which also have analogs in the experimental absorption spectrum. We believe that the most appropriate rationalization of the observed vibrational activity, which does not exclude possible contribution of large oxygen clusters, is the presence of highly excited oxygen dimers. The frequency range corresponding to their principal vibrational transitions is very specific [7], and a good agreement with the experimental data is observed (Table 2).

Correlation of the temperature dependence of the optical density of dimeric oxygen states (Fig. 3) with the amount of desorbed oxygen [15] allowed us to estimate the concentration of these states and the corresponding molar absorption coefficients. As shown in Fig. 4, rise in temperature to 723 K is accompanied by nonmonotonic decrease of the optical density D_{1557} at a frequency corresponding to stretching vibrations of triplet oxygen molecules. Further rise in temperature leads to increase of the absorption intensity which attains its maximal value at 1000 K. Using the formula $\varepsilon_{1557} = (D_{1557}^{298K} - D_{1557}^{573\,K})/\Delta c_{O2}$, where Δc_O is the specific amount of oxygen (mol g^{-1}) desorbed in the temperature range from 298 to 573 K at a constant density of the absorbing layer (2 mg cm^{-2}), we determined the molar absorption coefficient $\varepsilon_{1557} = 1.96\times10^5$ g mol^{-1} = 7.84×10^4 cm^3 mol^{-1}. The concentration c_{O_2} at 298 K was estimated at 3.3×10^{-6} mol $cm^{-3} \approx 2\times10^{18}$ au cm^{-3}. The minimal value at 573 K corresponds to a concentration c_{O_2} of 8.3×10^{-7} mol $cm^{-3} \approx 5\times10^{17}$ au cm^{-3}.

The temperature dependence of the optical density at the absorption maximum characteristic of the main vibrational transition in singlet oxygen molecules ($^1\Delta_g$, Fig. 2) displays two maxima at 573 and 1173 K. The molar absorption coefficient ε_{1457} is 2.68×10^5 g mol^{-1} or 1.07×10^5 cm^3 mol^{-1}, the minimal concentration of singlet oxygen molecules is $c_{O_2}{}^1 = 5.6\times10^{-7}$ mol cm^{-3} or 3.4×10^{17} au cm^{-3}, and the maximal concentration is $c_{O_2}{}^1 = 1.7\times10^{-6}$ mol cm^{-3} = 1.1×10^{18} au cm^{-3}. Comparison of the thermal desorption curves and temperature dependences of the oxygen concentrations shows that the maximal desorption corresponds to minimal concentration and vice versa [15]. The position of the concentration minima with respect to temperature coincides with the maximal intensity of the luminescence bands (Fig. 2).

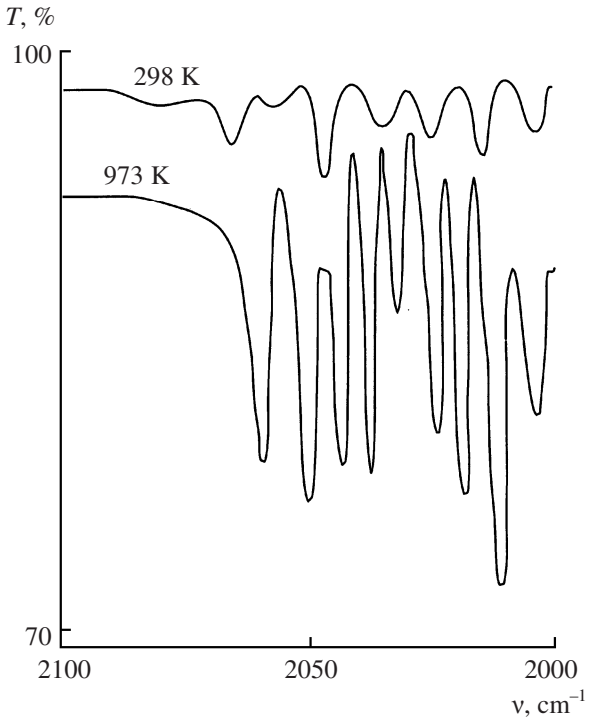

Fig. 4. Spectrum of highly excited molecular states of oxygen (O_2) in the structure of A-300 aerosil.

The high-temperature spectra are characterized by enhanced resolution and increased intensity of the absorption band in the region 769–775 cm^{-1}, corresponding to highly excited states of dimeric oxygen, $^1\Sigma_u^-$ (4 eV) and $^3\Sigma_u^+$ (4.5 eV) [7]. The temperature dependence of the optical density has two

Table 2. Vibrational transition frequencies in the system of electronically excited oxygen dimers

Therm	Energy, cm^{-1}	Experimental frequency, cm^{-1}	Data of [14], cm^{-1}
D $^3\Sigma_u^+$	75260	1920	1918
F $^3\Pi_u$	85689–87510	2003	2000
		2010	2001
		2015	2008
$^1\Pi_u^g$	86604	2023	2048
		2030	
		2035	
		2038	
		2040	
		2044	
e' $^3\Delta_{2u}$	74915	2049	2052
f $^1\Delta_{2u}$	86846	2053	2062

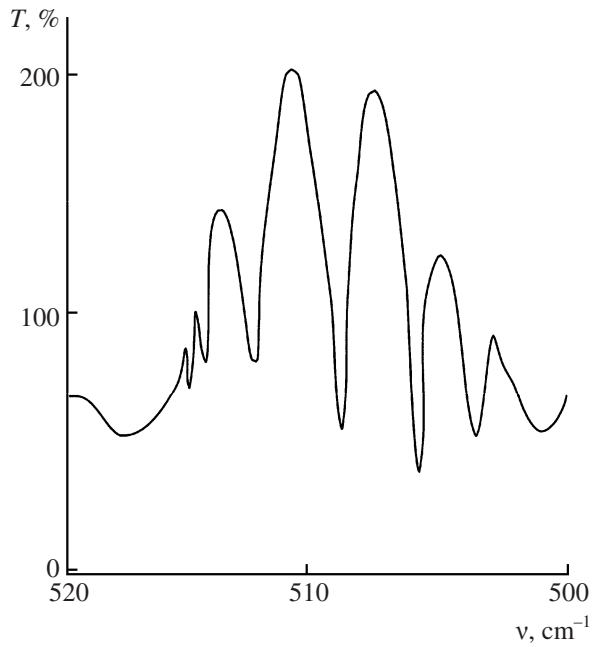

Fig. 5. Absorption bands in the region of vibrational activity of the Si–Si free oscillator ($^3\Sigma_g^+$, ν 507 cm^{-1}). *T* stands for transmittance.[2]

maxima at 573 and 973 K (Fig. 3). Using the corresponding molar absorption coefficient, the concentrations of the excited states were estimated as follows: $c_{\Sigma u}^{573} = 3.1\times10^{-6}$ mol cm^{-3} $= 1.9\times10^{18}$ au cm^{-3}, $c_{\Sigma u}^{773} = 1.8\times10^{-6}$ mol cm^{-3} $= 1.1\times10^{18}$ au cm^{-3}. The high concentrations of highly excited states of small associates suggest possible formation of condensed phases like exciton liquids with biexciton as structural unit [4].

The spectrum recorded at 573 K contains a series of very strong absorption bands in the region 520–500 cm^{-1}, which were assigned to the principal transitions in the isolated Si–Si bond system [7]; the envelope curve constitutes the luminescence band (Fig. 5). The centroid of the band (510 cm^{-1}) approaches a frequency corresponding to the enthalpy of condensation of molecular oxygen (544 cm^{-1}). In the low-frequency region typical of the minimal exciton bond energy and local electronic levels of excitons in the forbidden zone [6], we observed strong luminescence bands at 275 and 251 cm^{-1}, arising from the stationary excited state relaxation process, which could be interpreted as an indication of the formation of Coulomb bonds in the systems of their electron [Si–Si]$^-$ and hole components $[O_2]^+$. The first band is characterized by the presence of a satellite peak at 271.5 cm^{-1}, whose frequency exactly matches the principal transition in the electronically excited state ($^3\Sigma_u^-$, E_{ex} = 3 eV) of isolated Si–Si bond [7]. The luminescence intensity in the region 520–500 cm^{-1} increases at 973 K, and the luminescence band looks like a narrow peak at 515 cm^{-1}. The concomitant absorption bands due to isolated Si–Si bonds also reach their maximal intensity (Fig. 4). In the region 600–520 cm^{-1}, a well resolved series of stron absorption bands appears; it includes lines belonging to the first excited state of Si–Si bond ($^3\Pi_{u,i}$, $E_{ex} \approx 2$ eV) at 545 cm^{-1}. In addition, strong narrow luminescence peaks at 419, 332, and 266 cm^{-1} are present.

The validity of the results of spectral identification of the chemical structure of excited states and associates and especially of their cooperative interaction processes may be verified by analyzing temperature dependences of the heat capacity and magnetic susceptibility of the examined samples. By studying magnetic susceptibility of samples of silica gel in the temperature range from 298 to 1273 K we succeeded in revealing ordering processes and the existence of at least two types of cooperative states. As follows from the plots shown in Fig. 6, the general tendency is increase in the diamagnetic response with rise in temperature. States of the first type are characterized by a local maximum of diamagnetic response at 600 K, and those of the second type, at 1000–1100 K.

Decrease of the size of A-300 aerosil and KSK-2.5 silica gel particles to a level typical of Wannier–Mott type excitons (~100 Å) is accompanied by increase of the absolute diamagnetic susceptibility by almost an order of magnitude as compared to quartz. Therefore, the observed diamagnetic response may be attributed to formation of exciton condensate. The stability of temperatures at which the magnetic susceptibilities reach their extreme values indicates general character of the observed effect. The magnetic structure of exciton dielectric (or exciton liquid) corresponds to orbital (non-spin) antiferromagnetism of collectivized (Bloch) electrons [5] and is characterized by diamagnetic response to external magnetic field, which may be anomalously high for heterogeneous systems (superdiamagnetism). Estimation of the true specific diamagnetic susceptibility of the condensed phase of exciton states on the basis of their concentration (~10^{-6} mol g^{-1}) gives an anomalously high magnitude of $\chi_{ex} \approx$ (–) 1–10 cm^3 g^{-1}. The same conclusion can be drawn for disperse SiO_2 (χ = –10–50 cm^3 g^{-1}) with no

[2] As in Russian original.

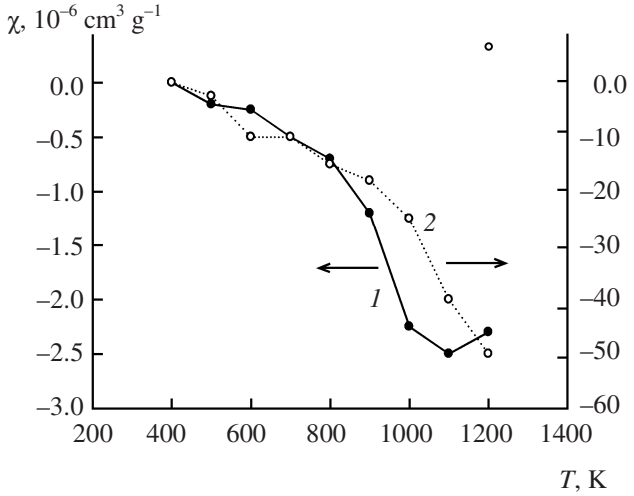

Fig. 6. Temperature dependences of the magnetic susceptibility of (*1*) quartz glass and (*2*) A-300 aerosil.

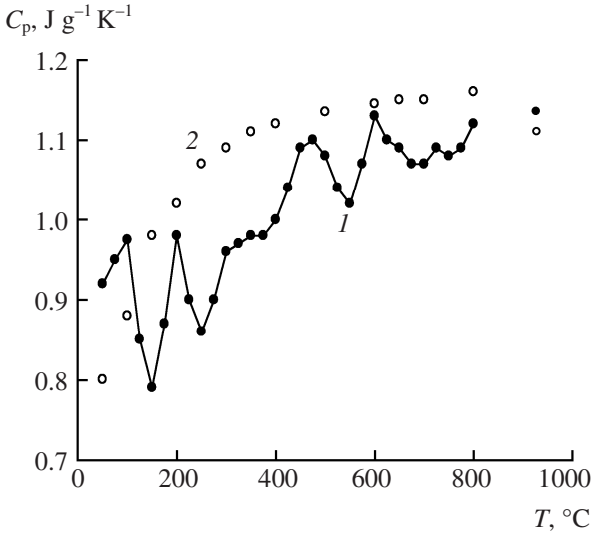

Fig. 7. Temperature dependences of the heat capacity of KSK-2.5 silica gel: (*1*) experimental and (*2*) calculated plots.

account taken of the concentration of exciton states, for pure silicon has a diamagnetic susceptibility χ of about –0.228 $cm^3\ g^{-1}$ [16].

Thus the character and shape of the temperature dependence of magnetic susceptibility confirm the role of the particle size in the formation of stable condensed phases of electronically excited states in the silica gel structure and make it possible to estimate the critical temperatures for heterogeneous exciton liquid–gas subsystem. The latter correspond to the position of the principal minima on the oxygen thermal desorption curves [15].

The results of numerous studies on the enthalpy and heat capacity of vitreous silicon dioxide at temperature above 298 K are fairly contradictory [17]. The deviations can attain ~10%, and there are no commonly accepted views on the reason for such deviations. However, the most probable reason may be nonidentity of the examined samples and their thermal histories. Comparison of our results with those obtained by calculations according to the Debye model [18] shows that the experimental dependence (step 50°C) is nonmonotonic (Figs. 7, 8). Most part of the heat capacity values of silica gel appear below the Debye curve (Fig. 7). In the case of quartz glass, the temperatures 200, 600, and 770°C can be distinguished (Fig. 8), at which relative excess of heat capacities is observed. These values coincide with the positions of maximal thermal emission of singlet oxygen [15], and the absolute excess of the heat capacity correlates with the thermal emission peak intensity. The temperature dependences of C_p for single-crystalline quartz and quartz glass are fairly similar (Fig. 8), but the former has a strong maximum at 550°C, which is known [1] to correspond to the second-order phase transition (α → β). Silica gel does not exhibit pronounced thermal emission in the above temperature range [15]. Insofar as in the latter case the diamagnetic response exceeds that observed for quartz glass by an order of magnitude, we can conclude that the low thermal

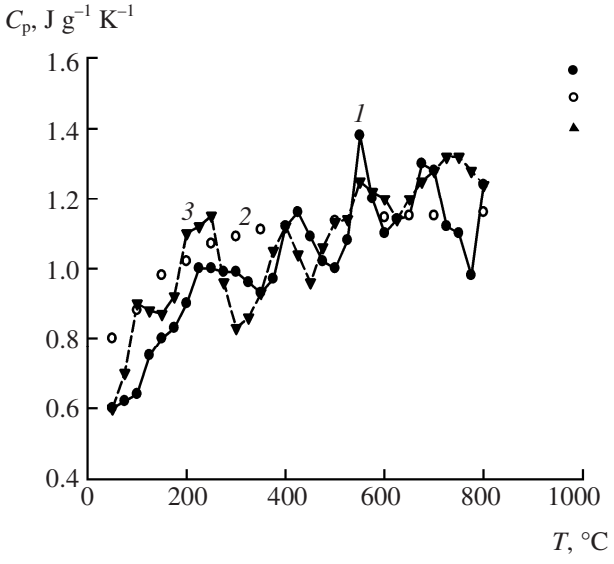

Fig. 8. Temperature dependences of the heat capacity of (*1*) quartz glass and (*2*, *3*) single-crystalline quartz: (*1*, *3*) experimental and (*2*) calculated plots.

capacities result from extensive condensation of electronically excited states, i.e., formation of exciton liquid. Obviously, evaporation of the condensate should be accompanied by accumulation of electronically excited states in the cationic sublattice of SiO_2 and by thermal emission of oxidized electronically excited components of the anionic sublattice (singlet oxygen molecules). Accumulation of electronically excited defects, i.e., appearance of an additional energy reservoir in a phase state which does not hamper heat exchange with the environment is reflected as excess heat capacity.

Thermal excitation → Distortion of structural polyhedrons → Vibronic interactions → Electronic excitation (loosening) of bonds

↓

Intramolecular redox reactions

↓

Accumulation of electronically excited states

Homolytic dissociation of bonds, oligomerization, polymerization, and thermal desorption $n[SiO_4]^{4-} \rightarrow [SiO_3]_n^{3-} + nO \rightarrow n/m\ O_m;\ m = 2, 3, 4 \ldots n$

Intramolecular rearrangements $n[SiO_{4/2}]^{4-} \rightarrow [SiO_{4-m/2}]_n^{4-}$; $m = 0, 1, 2, 3, 4.\ n \geq 3;\ m = 1 \rightarrow [SiO_{3/2}]_4^{8-}$:

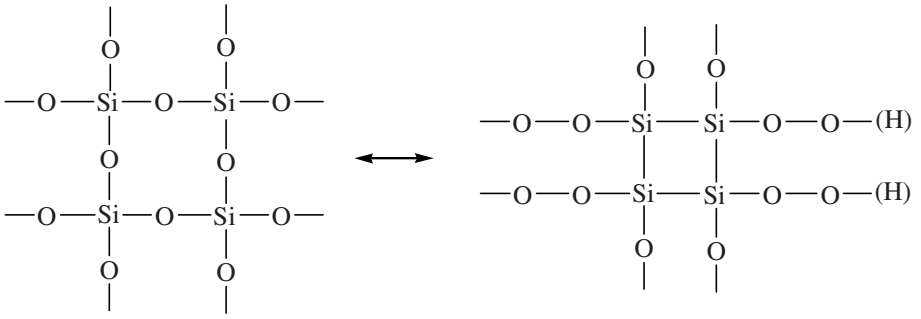

Thus the obtained results allow us to represent thermal evolution of the chemical structure of silicon oxides as a redox process initiated by thermal excitation and accompanied by homolytic dissociation of the skeleton bonds and intramolecular rearrangements. Thermal generation of electronically excited states, as well as thermal decomposition and desorption, leads to structure stabilization due to clusterization of these states and cooperative interactions.

EXPERIMENTAL

The spectral studies were performed using high-resolution (~0.01 cm^{-1}) IKS-25M, Chromex (USA), and Shimadzu-8400S FTIR spectrometers and a Chromex Wisard 1200 (USA) Raman spectrometer. The following silicon dioxide samples were used as substrates: ultrapure A-300 aerosil, KSK-2.5 silica gel, quartz glass plates, and synthetic single-crystalline quartz plates. The vibrational spectra were recorded from dispersed samples applied to a thin mica film (l ~ 5 μm). The controlled surface density was 1–2 mg cm^{-2}. Samples were subjected to thermal treatment at 20–900°C with a step of 100 deg (90 min) in dry purified air under atmospheric pressure. The spectra were recorded at a required temperature with digital compensation of the background signal with respect to a pure mica film whose spectrum was recorded under the same conditions. The average heat capacities were measured by drop calorimetry [19]. The magnetic susceptibilities were determined by the magnetic compensation technique using Hall sensors [20].

REFERENCES

1. Pryanishnikov, V.P., *Sistema kremnezema* (Silica Gel System), Leningrad: Stroiizdat, 1971, p. 298.
2. Radtsig, V.A., *Khim. Fiz.*, 1995, vol. 14, no. 8, p. 125.
3. Kopylov, V.B. and Pushkar', I.V., *Russ. J. Gen. Chem.*, 2006, vol. 76, no. 10, p. 1531.
4. Kulakovskii, V.D., Pikus, G.E., and Timofeev, V.B., *Usp. Fiz. Nauk*, 1981, vol. 22, p. 237.
5. Keldysh, L.V., *Usp. Fiz. Nauk*, 1970, vol. 100, p. 514.
6. Knox, R.S., *Theory of Excitons*, New York: Academic, 1963.
7. Huber, K.P. and Herzberg, G., *Molecular Spectra and Molecular Structure. IV. Constants of Diatomic Molecules*, New York: Van Nostrand Reinhold, 1979.
8. Tolstoy, V.P., Chernyshova, I.V., and Skryshevsky, V.A., *Handbook of Infrared Spectroscopy of Ultrathin Films*, Hoboken, NJ: Wiley, 2003.
9. Kopylov, V.B., Aleksandrov, K.A., and Sergeev, E.V., *Russ. J. Gen. Chem.*, 2007, vol. 77, no. 6, p. 1002.
10. Laskorin, B.N., Strelko, V.V., Strazhesko, D.N., and Denisov, V.I., *Sorbenty na osnove silikagelya v radiokhimii. Khimicheskie svoistva. Primenenie* (Silica Gel-Based Sorbents in Radiochemistry: Chemical Properties and Application), Moscow: Atomizdat, 1977.
11. Lunin, V.V., Popovich, M.P., and Tkachenko, S.N., *Fizicheskaya khimiya ozona* (Physical Chemistry of Ozone), Moscow: Mosk. Gos. Univ., 1998.
12. Schumb, W.C., Satterfield, C.N., and Wentworth, R.L., *Hydrogen Peroxide*, New York: Reinhold, 1955.
13. Tertykh, V.A. and Belyakova, L.A., *Khimicheskie reaktsii s uchastiem poverkhnosti kremnezema* (Chemical Reactions Involving Silica Gel Surface), Kiev: Naukova Dumka, 1991.
14. Razumovskii, S.D., *Kislorod. Elementarnye formy i svoistva* (Oxygen. Elemental Forms and Properties), Moscow: Khimiya, 1979.
15. Kopylov, V.B., Loseva, N.I., and Pak, V.N., *Zh. Prikl. Khim.*, 1996, vol. 69, no. 1, p. 926.
16. *Fizicheskie velichiny. Spravochnik* (Physical Quantities. Reference Book), Grigor'ev, S.I. and Meilikhov, E.Z., Eds., Moscow: Energoatomizdat, 1991.
17. Gurvich, L.V., Veits, I.V., and Medvedev, V.A., *Termodinamicheskie svoistva individual'nykh veshchestv* (Thermodynamic Properties of Pure Substances), Moscow: Nauka, 1979, vol. 2, book 1.
18. Landau, L.D. and Lifshits, E.M., *Statisticheskaya fizika* (Statistical Physics), Moscow: Nauka, Fizmatlit, 1995, part 1.
19. Arkhipov, V.A., Dobretsov, V.N., Perkatova, L.S., and Ustinov, V.A., *Zh. Fiz. Khim.*, 1975, vol. 19, no. 5, p. 1329.
20. Kopylov, V.B. and Sergeev, E.V., *Tech. Phys. Lett.*, 2007, vol. 33, no. 8, p. 670.